We are IntechOpen, the world's leading publisher of Open Access books Built by scientists, for scientists

4,800
Open access books available

122,000
International authors and editors

135M
Downloads

Our authors are among the

154
Countries delivered to

TOP 1%
most cited scientists

12.2%
Contributors from top 500 universities

CLARIVATE ANALYTICS BOOK CITATION INDEX INDEXED

WEB OF SCIENCE™

Selection of our books indexed in the Book Citation Index in Web of Science™ Core Collection (BKCI)

Interested in publishing with us?
Contact book.department@intechopen.com

Numbers displayed above are based on latest data collected.
For more information visit www.intechopen.com

7

The Role of Ultrasonography in the Assessment of Arterial Baroreflex Function

Yu-Chieh Tzeng
Cardiovascular Systems Laboratory
University of Otago
New Zealand

1. Introduction

Cardiovascular disease is the leading cause of mortality in the developed world [1]. Experimental research indicates that in addition to traditional risk factors such as hypertension and dyslipidemia, dysfunction of the autonomic nervous system is also a powerful independent risk factor for death from cardiovascular disease. Although not yet routinely assessed in clinical practice, depressed baroreflex function increases the risk of death following myocardial infarction [2], in chronic heart failure [3], and recent trials also clearly indicate an increased risk for both ischemic and hemorrhagic stroke [4, 5]. In the context of these morbid epidemiological correlations, it is not difficult to justify the need for a better understanding of the mechanisms and factors involved in normal human baroreflex regulation.

Ultrasonography has played a vital role over the past decades not only in clinical medicine but also in advancing our understanding of fundamental biological processes. This proposition is certainly true for human cardiovascular research, where the non-invasive nature of ultrasonography has enabled physiologists and clinicians to study regulatory mechanisms that could otherwise only be examined in animal models under sedation or anaesthesia. The aim of this chapter is to review the pivotal role that ultrasonography has played in advancing our understanding of human baroreflex function. The chapter will begin with an overview of the human baroreflex in section 2 with particular emphasis on cardio-vagal regulation of the heart, and vascular sympathetic regulation of peripheral vascular resistance. Section 3 will introduce the technical application of ultrasonography in baroreflex research with emphasis on the use of B-mode imaging in the evaluation of the mechanical and neural components of the baroreflex arc. Important practical, analytical, and physiological considerations will be discussed. Finally, the literature will be reviewed in section 4 to illustrate how the practical application of vascular ultrasound imaging has lead to deeper insights into the workings of the human baroreflex not otherwise possible.

2. Physiology of the baroreflex

The arterial baroreflex is critical to both short and long term regulation of blood pressure. The sensory components of this reflex comprise of stretch sensitive nerve endings situated

in vessel walls of some arteries, particularly in the carotid sinus and the aortic arch that respond to changes in vascular distention pressure by altering afferent discharge activity in the carotid sinus nerve (a branch of the glossopharyngeal nerve) and the aortic nerves.

Afferent baroreceptor inputs project to regions of the nucleus tractus solitarius, which extends almost over the entire length of the medulla and is the exclusive first relay station and integration area for afferent baroreceptor information [6]. Numerous inter-connections exist between the nucleus tractus solitarius and other structures important in the baroreflex, including the hypothalamus, amygdala, parabrachial nuclei, subfornical organ, cerebellum, and rostral ventrolateral medulla [7]. However, the precise central interneuronal connections that drive parasympathetic and sympathetic motoneurons, and the locations of vagal-cardiac motoneurons have not been located in humans. In animals they are found in variable locations, including the nucleus ambigus in the cat [8], and dorsal motor nucleus of the vagus in dogs and monkeys [9]. Sympathetic pre-ganglionic motoneurons are located in the intermediolateral column of the spinal cord [10]. Irrespective of the precise central neuronal connections mediating the baroreflex, it is clear that the end effector response to arterial baroreflex stimulation is an increase in efferent vagal activity, and a decrease in efferent sympathetic activity [11].

The efferent limbs of the baroreflex can be functionally considered as consisting of a cardiac component and a vascular component. The cardiac baroreflex refers to the prompt adjustment of heart rate, stroke volume (and therefore cardiac output) in response to changes in blood pressure. These responses are mediated primarily via the vagus nerve because they are markedly attenuated following surgical vagotomy and muscarinic cholinergic [12]. In healthy humans at rest, and during exercise, the cardiac baroreflex can respond rapidly with cardiac period intervals beginning to adjust within 0.5 sec following baroreceptor loading with neck suction [13]. Although maximal responses increase with advancing age, in the young, they generally takes place within 3-4 seconds following baroreceptor loading, and 2-3 sec following baroreceptor unloading respectively in the young [14]. Reflex alterations in heart rate can also arise due to the action of the sympathetic nervous system. Increased sympathetic activity can increase heart rate via the release of noradrenalin in postganglionic nerve terminals, or the release of adrenaline into the systemic circulation from the adrenal medulla. It is important to recognize that whereas the chronotropic response of the heart to baroreflex stimulation is dominated by vagal activity (via the release of acetylcholine), the inotropic responses to baroreflex stimulation responsible for changes in stroke volume are mediated via the sympathetic nervous systems.

In contrast, the vascular baroreflex refers to regulation of peripheral vascular smooth muscle tone. The major site of vascular resistance is thought to reside in the arterioles and capillaries, which in the systemic circulation are densely innervated with post-ganglionic sympathetic fibers. Although sympathetic regulation of venous tone is not a key determinant of peripheral vascular resistance, venous constriction influences blood volume distribution. The reaction times of the vascular sympathetic baroreflex are slower compared to cardiac responses. Even though changes in sympathetic nerve activity can occur with latencies of ~200ms after changes of afferent nervous activity to the central nervous system, the lag times associated with sympathetic neurovascular transduction at the level of the neuromuscular junction are substantially longer such that the first changes

in end organ response are seen only after 2-3 seconds. The maintenance of blood pressure therefore requires the effective regulation and integration of both the cardiac and vascular baroreflex arc.

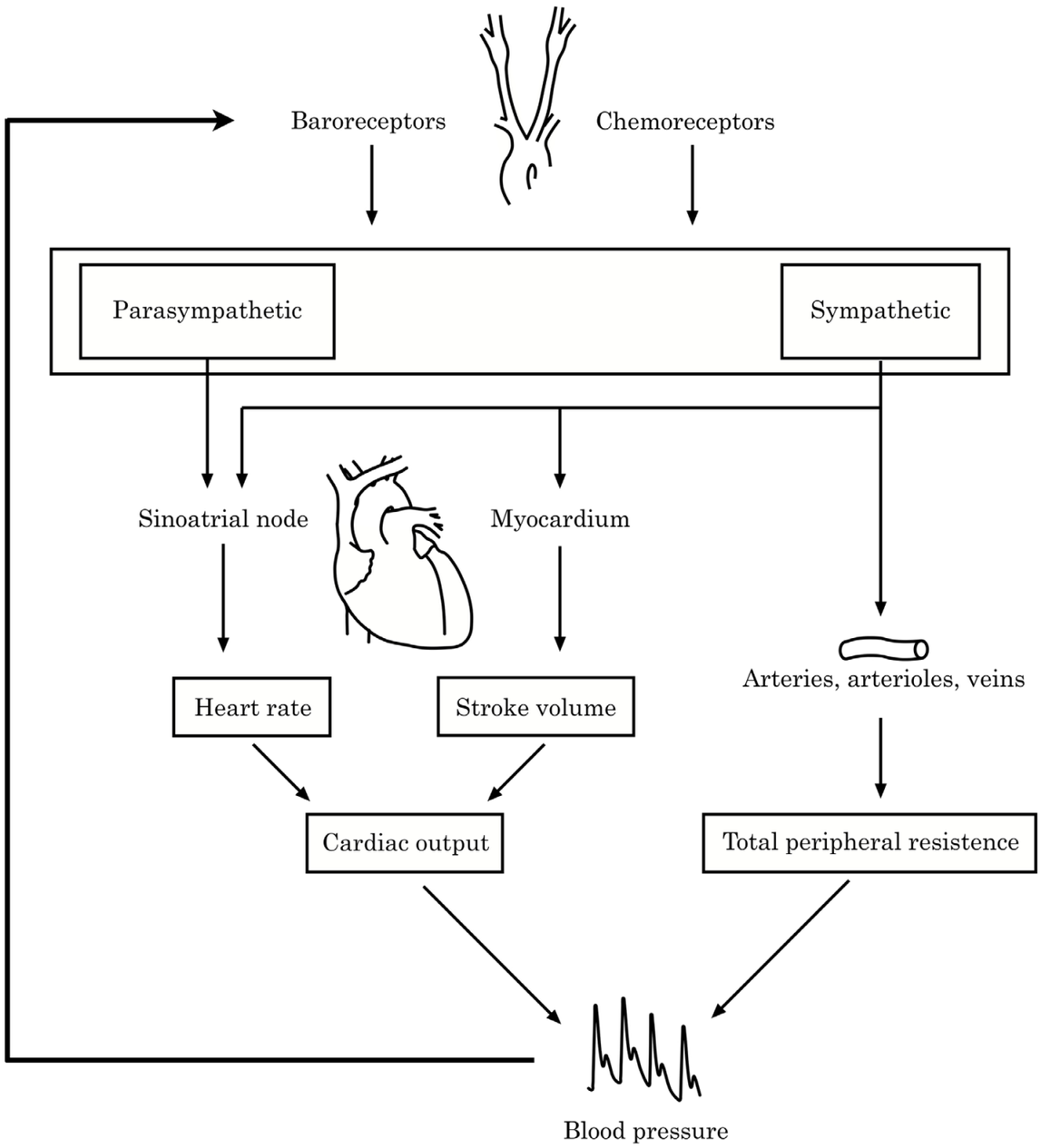

Fig. 1. Schematic showing the major mechanistic pathways involved with short-term systemic blood pressure control. Note that in vivo the baroreflex arc is a closed-loop system.

3. Assessment of the mechanical and neural components of the cardiac baroreflex

3.1 Overview

Baroreflex gain has traditionally been quantified as the relation between changes in arterial blood pressure and cardiac period (R-R intervals), heart rate, or sympathetic nerve activity. This analysis assumes that blood pressure is the input that drives reflex autonomic changes. However, baroreceptors respond to mechanical deformation and not the pressure *per se*. Therefore, the transduction of blood pressure into barosensory stretch, and the consequent transduction of barosensory stretch into efferent parasympathetic and sympathetic neural outflow are critical steps that determine the integrated baroreflex response. The major contribution of vascular ultrasound imaging to baroreflex research has been the enabling of these critical components of the integrated baroreflex arc to be studied separately and non-invasively in humans through the use of B and M-mode imaging processes [15].

In principal, the imaging analysis can be combined with any baroreflex assessment technique provided adequate ultrasound images can be obtained. In practice, however, apart from the modified Oxford method, the approach has only been successfully applied in subjects performing the Valsalva maneuver [16] and under steady state resting conditions using linear transfer function analysis [17]. Therefore, considering the relative novelty of the approach, and the fact that no method can be considered the gold standard, investigators wishing to undertake this form of analysis should choose their approach based on their unique experimental requirements, and an understanding of the analytical and theoretical shortcomings of each method. In this section, methods that are *technically* suitable for this form of analysis from an imaging perspective will be presented in context of some of these considerations. Beyond the scope are methods that do not permit the accurate acquisition of carotid images (e.g. neck suction/pressure, dynamic squat-stand maneuvers) and techniques based on highly controversial physiological assumptions (e.g. spontaneous sequence method, high frequency transfer function gain) [18, 19].

3.2 Carotid ultrasound scanning protocol

The assessment begins with the identification of wall boundaries, which appear as parallel echogenic lines separated by a hypoechonic space in longitudinal B-mode image (figure 2). Although the internal carotid, bulb, and common carotid arteries can all be imaged (figure 3), the latter generally yields the best image quality because the vessel course is parallel to the surface of the skin and is positioned at right angles to the ultrasound beam. The first echo along the far wall corresponds to the lumen-intima interface whilst the second and normally brighter echo corresponds to the media-adventitia interface. The echolucent zone in between corresponds to the media. It is important to recognize that interfaces may be difficult to discern when the near and far walls of the vessels are curvilinear and not at right angels to the ultrasound beam. Therefore, within the carotid bulb where the walls flare and dilate, or along the proximal internal carotid where the walls do not lie in parallel, only short segments of wall may be seen on a single frame. For these reasons, vascular distention waveforms are generally acquired 1-2cm of the bifurcation even though baroreceptor density is greatest at the carotid bulb. Other causes for the loss of wall interface that are unrelated to scanning technique include the presence of atherosclerotic plaques or the presence of fat in the arterial wall.

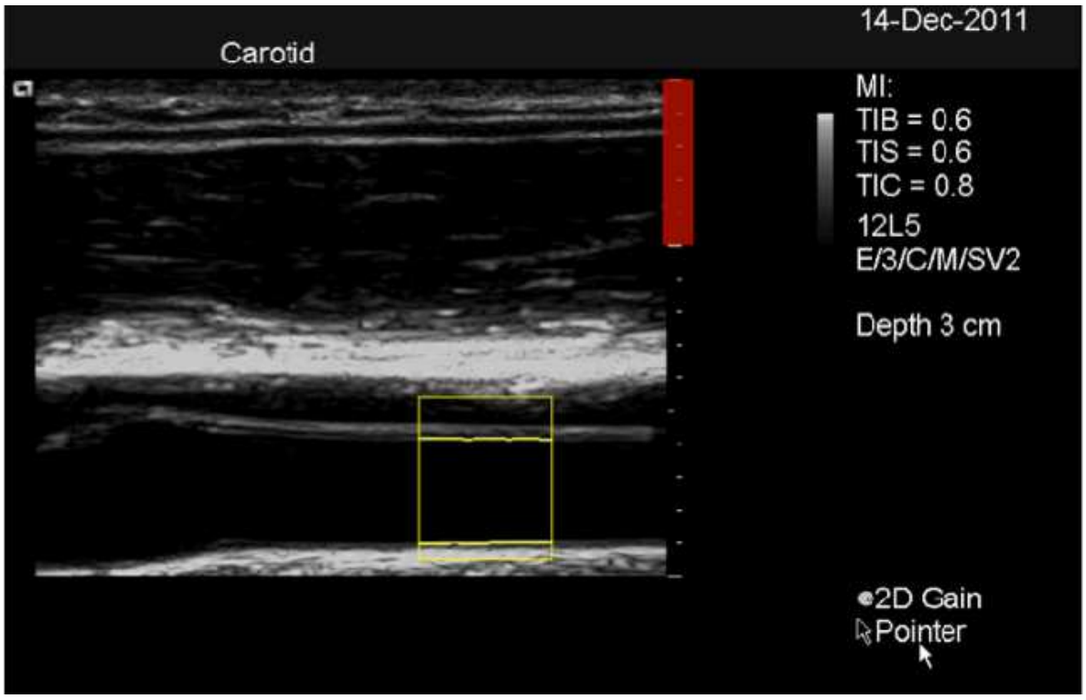

Fig. 2. Sample screen shot showing the custom edge tracking of the carotid luminal diameter.

Studies are conducted using linear array probes (7.5-13 Mhz) with the subjects head tilted ~45º away from the side of the study to capture a longitudinal section of the common carotid artery ~1 cm proximal to the bifurcation. This usually requires an initial cursory scan to orient the sonographer to the subject's carotid anatomy to establish the site of the bifurcation and to differentiate between the internal and the external the external carotid artery. Upon identifying the distance common carotid immediately proximal to the bulb, the probe should be manipulated to optimize the view of the arterial wall such that the lumen-intima and media-adventitia interfaces over a 1-cm length can be clearly displayed. Images should be captured as close to a 45 degrees angle as possible and both the near and far walls should be clearly visible for robust analysis.

The continuous digital video screen shot of the optimized B-mode images are then recorded and saved for offline analysis using custom written edge-tracking software (figure 2). The region of interest is calibrated for length, and using a pixel-density algorithm the vessel walls are tracked and diameter measured at 30 Hz resolution for the entire video that encompassed the Oxford trial. In contrast to methods originally described by Hunt et al., where hardware limitations meant that image sets could only be acquired on approximately every other cardiac cycle, our technique enables the carotid diameter data to be acquired for every cardiac cycle throughout the duration of the baroreflex test (~3 minutes). High resolution tracking of carotid distension waveforms can also be obtained using a number of commercially available systems that employ interlaced M-mode and B-mode imaging, such as the ART.Lab system (Esaote, Maastrict) or the QFM-21 (Haedco, Japan). However, the use of A-mode imaging with the QFM-21 limits the utility of this device given there is no visual feedback in B-mode to guide the accurate placement of the probe relative to the length of the carotid artery.

Method	Strength	Weaknesses
Modified Oxford method	Partial open loop analysis of baroreflex gain Not confounded by differences in respiration rate Enables the assessment of baroreflex hysteresis Evaluate cardiac baroreflex gain as well as the neural arc of the smpathetic baroreflex	Invasive procedure require venous cannulation Potential influence of drugs on vascular transduction Does not permit evaluation of sympathetic neurovascular transduction given the use of vasoactive drugs Subjectivity of analysis
Valsalva manuever	Non-invasive Non-pharmacological Partial open loop analysis of baroreflex gain Enables the assessment of baroreflex hysteresis Evaluate both cardiac and symaptethic baroreflex function	Need for subject compliance Poor consistency across subjects
Spectral methods	Non-invasive Non-pharmacological Does not permit assessment of baroreflex hysteresis Prone to confounding by changes in respiration	Liable to confounding by non-baroreflex mediated fluctuations in vagal outflow (e.g. respiration) Controversial physiological assumptions Closed-loop analysis

Table 1. Comparison of methods for the assessment of baroreflex function

3.3 Overview of techniques and data analysis

The following overview summaries the data analysis that is involved in the quantification of integrated, mechanical and neural baroreflex gains. Only methods involving general linear regression and linear transfer function analysis will be outlined. Higher order mathematical models of baroreflex function fall outside the scope of this chapter.

The modified Oxford method

In 1969 Smyth et al., proposed a method for assessing arterial baroreflex gain that involved regressing reflex cardiac interval responses to systolic blood pressure changes induced with vasoactive drugs [20]. Commonly referred to as the 'Oxford method', this technique has become widely regarded as the gold standard measure of baroreflex function. Although the assessment was originally carried out using bolus injections of angiotensin, the method has undergone many incremental modifications since its introduction. These include, for example, the use of drugs with minimal direct cardiac chronotropic effects, and the administration of vasodilator and vasoconstriction drugs in sequence to enable the complete characterization of both the cardiac and sympathetic baroreflex function (modified 'Oxford method').

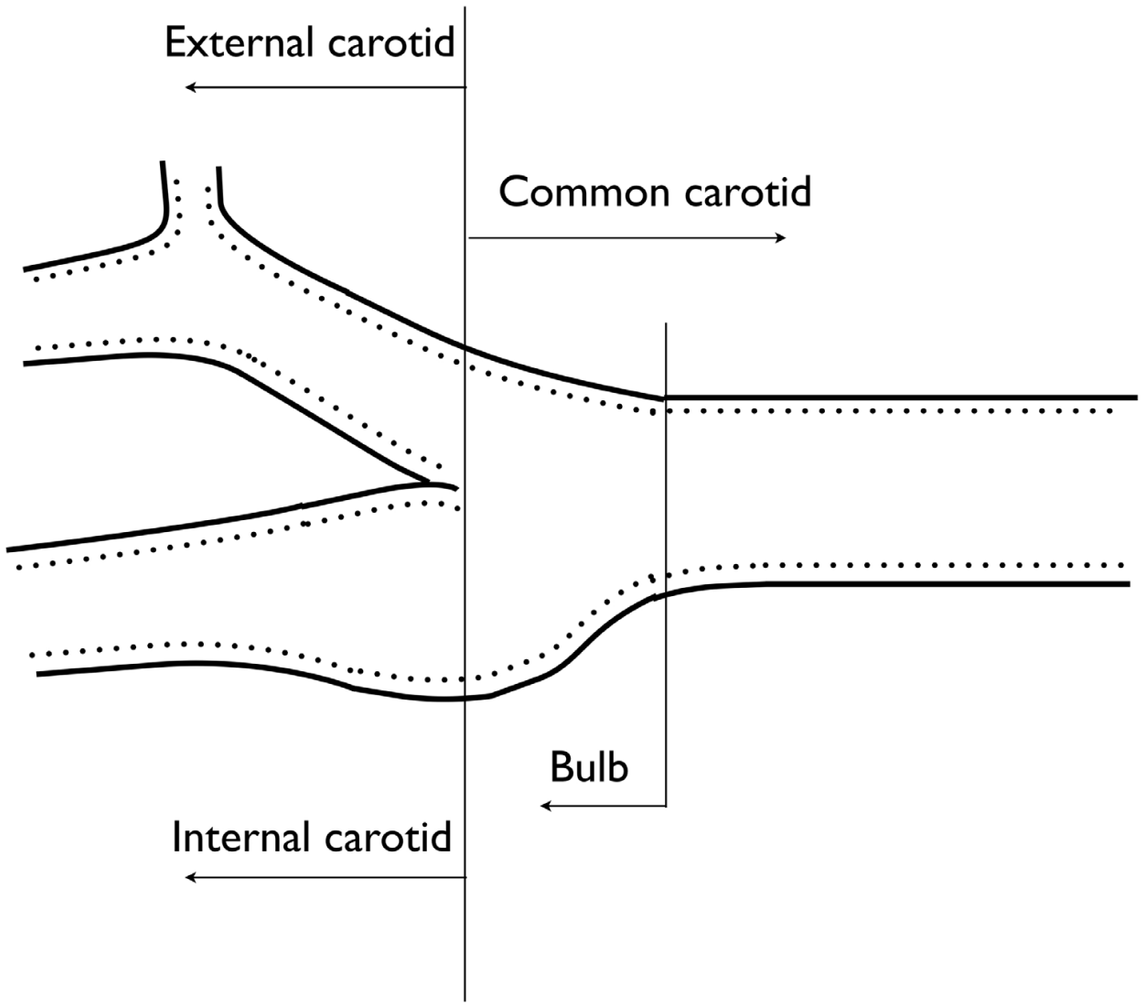

Fig. 3. Schematic showing the common, internal and external carotid arteries. The carotid bulb can be recognized in most subjects as the site where common carotid dilates slightly and the vessel walls flare out such that they're no longer parallel to each other. The elliptically shaped bulb is geometrically complex in the longitudinal view and therefore can be difficult to image in its entirety within a single frame. The external carotid artery lies anterior and medial to the internal carotid in 90% of subjects but is reversed in the remaining 10%. The internal carotid artery is generally larger than the external carotid, and has no braches as it ascends into the skull to supply the brain, whereas the external carotid has branches that supply the neck and face.

A key advantage of the method is that blood pressure can be perturbed across a wide range within a sufficiently short time frame to *clearly* engage the baroreflex. This is a critical consideration given the baroreflex is a closed-loop system (figure 1) and accurate quantification of input-output relations in theory requires the loop to be opened. Whilst the open-loop condition cannot be meet under the majority of human experimental settings, the active perturbation of blood pressure does allow the loop to be partial-opened to yield robust estimates of baroreflex gain [21]. The key objection to the Oxford method relates to the use of vaso-active agents, which may exert unquantifiable effects on baroreceptor transduction, cardiopulmonary afferent activity and sinus node activity. However, the practical significance of these concerns remains unclear. Other strengths and weaknesses of the method are summarized in Table 1.

Technically the modified Oxford method involves sequential intravenous bolus injections sodium nitroprusside (SNP) and phenylephrine hydrochloride (PE). Once recordings of hemodynamic measurements have begun, blood pressure should be carefully monitored and allowed to stabilize, after which the injection of SNP can be administered. This should be followed ~60 seconds later by the injection of PE. Recording can cease when systolic blood pressure began to plateau after the rise after the PE injection. Oxford trials, therefore, typically last 120 to 180 seconds. Doses given for SNP and PE are typically 150 and 200g, respectively, although this should be adjusted on an individual basis if an insufficient blood pressure perturbation is achieved (systolic blood pressure change <15 mm Hg). It is common practice to account for known baroreflex delays, which can be done by matching systolic blood pressure values to either the concurrent heartbeat for R-R intervals >800 ms or a 1 beat delay for shorter heart periods (typically between 500 and 800 ms). Due to baroreflex hysteresis, baroreflex sensitivities should be calculated separately for SNP and PE injections to identify the gain (or sensitivity) against falling and rising blood pressure.

Figure 4 shows a representative tracing of heart rate, carotid artery lumen diameter, and finger blood pressure during a modified Oxford baroreflex test sequence. For the assessment of cardio-vagal BRS, the pressure to R-R interval relation for falling pressures are examined at the onset of the systolic blood pressure decrease, which typically occur ~30 sec after the bolus injection of SNP, and ends when systolic blood pressure reached its nadir. For rising pressures, data selection begins at the nadir in systolic blood pressure and end when pressure peaks after the bolus injection of PE.

It is common for the identification and elimination of the saturation and threshold regions to be done via visual data inspection [22, 23]. However, mathematical modeling procedures can be applied for more objective analysis. For example, a piecewise linear regression can be applied to the raw data points to statistically identify breakpoints that occur at the upper and lower ends of the data set (Figure 5) [24, 25]. Other approaches for the objective identification of cardiac-vagal BRS have been reported in the literature including the use sigmoid [26], logistic [27] and elliptical functions [28].

Typically, an arbitrary threshold for the correlation coefficient of the linear segment is set at 0.6 to justify the use of a linear regression model. It is also conventional to account for respiratory-related fluctuations in R-R interval and systolic blood pressure by averaging R-R

intervals or heart rate across 2 or 3 mm Hg bins. However, although data binning improves the correlation coefficients, neither respiratory rate [23] nor data binning [26] materially influence the magnitude of the gain estimates.

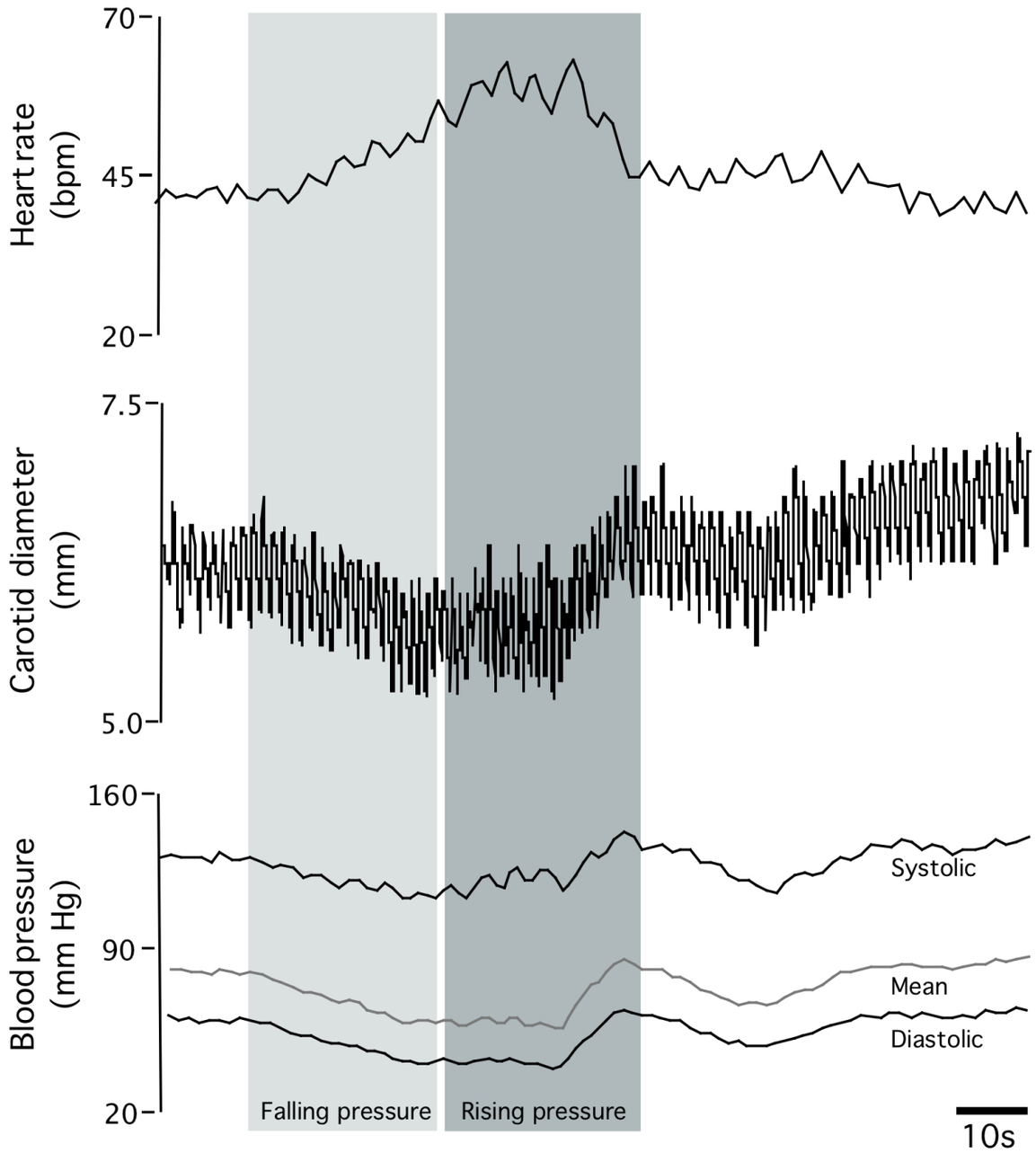

Fig. 4. Representative recording of a modified Oxford baroreflex test sequence. Intravenous bolus injections of sodium nitroprusside were followed ~60 s later by phenylephrine hydrochloride. The grey scale areas indicate the data segments typically taken for the determination of baroreflex gain.

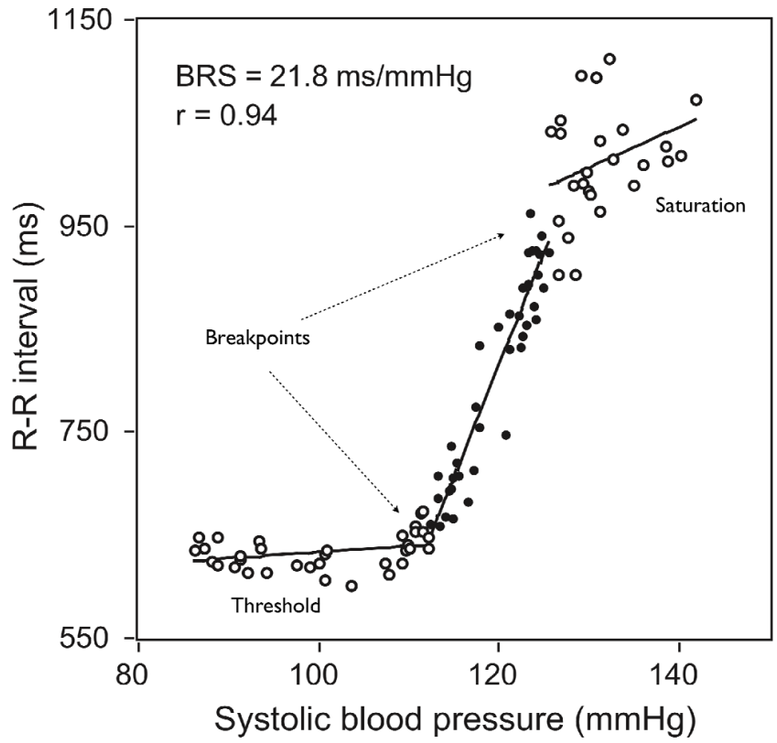

Fig. 5. Piecewise regression model for elimination of threshold and saturation regions of the integrated baroreflex response to rising pressures. Open circles (○) represent the threshold and saturation regions and the closed circles (●) represent the linear portion of the baroreflex gain. Arrows indicate breakpoints that separate the threshold, saturation, and linear region (Adapted from Taylor et al., 2011).

The gain of the mechanical and neural components can be calculated separately for both rising and falling pressures, with exclusion of the threshold and saturation regions as done for the assessment of integrated gain. For the mechanical component, systolic carotid lumen diameter measurements within a cardiac cycle should be plotted against systolic blood pressure, and for the neural component, R-R intervals or heart rate should be plotted against systolic carotid lumen diameter (figure 6).

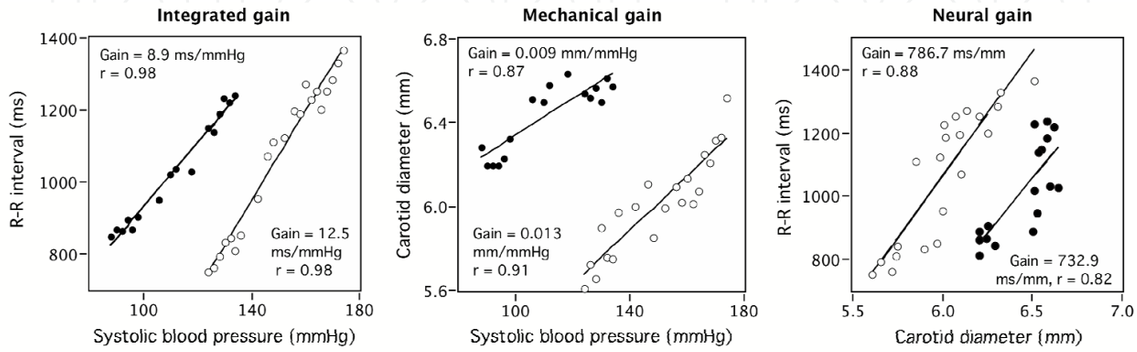

Fig. 6. Integrated, mechanical and neural gains for rising pressures in the morning (●) and afternoon (○) for one subject. (adapted from Taylor et a., 2011).

For assessment of integrated, mechanical, and neural components of the sympathetic baroreflex, simple linear regression procedures are generally applied but with few modifications. First, instead of systolic lumen diameters and systolic pressures, integrated and mechanical gains for the sympathetic arc are derived using diastolic lumen diameters and diastolic blood pressure. This is because diastolic pressure correlates more strongly to sympathetic activity, which in humans are generally recordings of muscle sympathetic nerve activity (MSNA) made in the peroneal nerve [29]. Second, sympathetic activity has a bursting pattern that rarely maintains a 1:1 relation with cardiac cycles even at low blood pressures where baroreflex-mediated sympatho-inhibition is low. Therefore, pharmacological baroreflex testing across a wide range of blood pressures invariably results in an over-representation of cardiac cycles with zero sympathetic activity. To account for this error, cardiac cycles can be weighted according to the presence or absence of observable sympathetic bursts. For example, cardiac cycles with zero's below the lowest pressure associated with a sympathetic burst are assigned a weight of 0 ('false' zero) whereas zeros above the highest pressure associated with a sympathetic burst were assigned a weight of 1 ('true' zero) [30]. Some groups employ data binning (e.g. across 3mmHg blood pressure increments) to reduce the statistical impact of inherent beat-to-beat variability in nerve activity [31], which are generally represented as total integrated sympathetic activity (i.e. the product of burst frequency and average burst area in arbitrary units).

The Valsalva maneuver

The Valsalva maneuver was first described by Antonia Maria Valsalva in the 17th century as a method for testing the patency of the Eustachian tube. However, the maneuver has gained subsequent acceptance as a means of stressing the baroreflex due to its well-characterized effects on cardiac output, venous return, and blood pressure. Essentially the maneuver involves forced expiration against a closed glottis, or a short tube to enhance expiratory resistance. Mouth pressure is measured and maintained at a constant level (e.g. 40 mmHg) for 15 seconds. Figure 7 shows the typical response in blood pressure and heart rate (MSNA not shown), which have been characterized into four phases. Phase one is the initial blood pressure rise and heart rate and MSNA reduction (via the baroreflex) due to a mild rise in stroke volume secondary to elevated intrathoracic pressure forcing blood out of the pulmonary circulation into the left atrium. The sustained elevation in introthoracic pressure

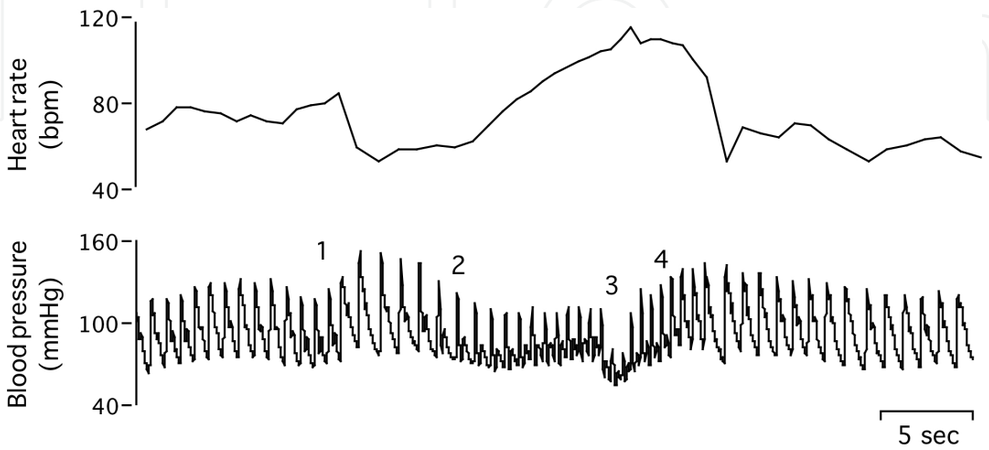

Fig. 7. Blood pressure and heart rate changes during the Valsalva manuver.

during phase two impedes venous return and consequently reduces cardiac output. This phase triggers a baroreflex mediated increase in heart rate and MSNA. Phase three commences with the pressure release and resumption of normal breathing. During this phase blood pressure decreases briefly as the external compression on the aorta is released and heart rate increases. This is followed by phase four as blood pressure starts to rise due to an increased in cardiac output secondary to a rapid increase in venous return, and the background of elevated sympathetic vascular resistance that occurred during phase two. During phase four, heart rate decreases and MSNA falls.

The regression approaches described for the modified Oxford method are also applicable to the Valsalva maneuver. In general, estimates of cardia-vagal baroreflex gain can be determined from both phase two or four of the response. However, satisfactory sympathetic baroreflex slopes may only be obtainable during phase two, given the relative paucity of sympathetic bursts during phase four [32].

Transfer function analysis

Integrated, neural, and mechanical baroreflex gains can be quantified using transfer-function analysis of spontaneously occurring low frequency (0.14-0.15 Hz) blood pressure, carotid lumen diameter, R-R interval, and normalized MSNA fluctuations. The data processing typically begins with interpolation (e.g. linear, spline) and re-sampling (1-4 Hz) of beat-to-beat systolic pressure, carotid lumen diameter, and R-R intervals to provide equidistant time series that are required for Fourier analysis. Due to noise inherent in finite data series, its common to apply the Welch averaging technique to minimize data variance in exchange for reduced frequency resolution. Welch averaging involves the subdivision of the entire data epoch into successive overlapping segments of equal lengths. The data within each window should be de-trended and passed through a Hanning window before spectral analysis. The frequency-domain transforms can be computed with a fast Fourier transformation algorithm. The transfer function H (*f*) between the two signals was calculated as:

$$H(f) = Sxy(f)/Sxx(f)$$

where S_{xx} (*f*) is the autospectrum of input signal and S_{xy} (*f*) is the cross-spectrum between the two signals. The transfer function gain $|H(f)|$ and phase spectrum $|\Phi(f)|$ were obtained from the real part H_R (*f*) and imaginary part H_I (*f*) of the complex transfer function:

$$|H(f)| = \{[HR(f)]2 + [HI(f)]2\}$$

$$\Phi(f) = \tan\text{-}1[HI(f)/HR(f)]$$

The squared coherence function MSC (f) was estimated as:

$$MSC(f) = |Sxy(f)|2/[Sxx(f)Syy(f)],$$

where S_{yy}(*f*) is the autospectrum of changes in output signal. Given that transfer function analysis is a linear methodology that is yields only valid gain estimates if the cross-spectral coherence is sufficiently high. This threshold is conventionally set at 0.5 although lower thresholds have been applied.

According to this approach, the integrated cardiac baroreflex gain corresponds to the average systolic pressure to R-R interval transfer function gain within the low frequency range (0.04-0.15) [33]. The mechanical component is the average transfer function gain between systolic blood pressure and systolic carotid diameter fluctuations whereas the neural gain is the average systolic carotid diameter to R-R interval transfer function gain within the same frequency range. In theory the transduction of carotid diameter fluctuations to changes in MSNA can also be assessed although details of these transfer function characteristics in humans have not yet been reported in the literature.

The major advantage of the spontaneous spectral approach is that the assessment can be made non-invasively without the use of drugs or special provocation maneuvers (the procedure becomes invasive if MSNA recordings are made). However, there are important potential shortcomings with this technique. First, because input and output relationships between the various haemodynamics parameters are assessed under spontaneous conditions, the derived transfer function parameters reflect close-loop relations that may not accurately reflex open-loop gains [34]. Furthermore, the technique is highly liable to confounding from respiratory influences. For example, fluctuations in R-R intervals associated with respiratory activity (respiratory sinus arrhythmia) can merge, accentuate, and confound the magnitude of low frequency fluctuations if breathing rate falls within the low frequency range (i.e.<0.15Hz) [23]. Such respiratory influences need to be carefully controlled for and may be minimized with the use of pace respiration.

4. New insights into baroreflex physiology gain through the application of vascular ultrasound

The technical advances described in section 3 offer the potential for more detailed understanding of mechanisms underlying changes in baroreflex function not previously attainable in health and disease [35]. The following is a summary of new insights into baroreflex physiology that have been gained with the aid of ultrasonography.

4.1 Baroreflex hysteresis

It is well recognised that cardiac baroreflex function exhibits hysteresis; baroreflex responses are greater for rising vs. falling blood pressures. Hysteresis is an intrinsic feature to the cardiac baroreflex, and is observable with both pharmacologically induced changes in blood pressure (Pickering et al. 1972; Bonyhay et al. 1997; Rudas et al. 1999) and direct neck pressure stimulation (Eckberg & Sleight, 1992). This pattern of hysteresis has classically been attributed solely to the visoelastic properties of barosensory vessels such that, for a given blood pressure, vessel diameters are greater if the pressure was on the ascent. However, Studinger et al., showed that hysteresis derives not only from barosensory vessel mechanics, but also from complex interactions with neural resetting which often offset the changes in mechanical gain [24]. These findings further reinforce the concept that the integrated baroreflex gain derives from the combined influences of mechanical transduction of pressure into baroreceptor stretch, and neural transduction of baroreceptor stretch into vagal outflow.

4.2 Baroreflex changes with aerobic exercise

Although baroreflex impairment is a strong predictor of adverse cardiac and cerebrovascular outcomes, very few interventions have been shown to successful ameliorate the decline in baroreflex function associated with aging and cardiovascular disease. Some data suggest that aerobic exercise training may enhance cardiac baroreflex function although the mechanisms underpinning these changes are poorly understood. Using the valsalva technique, Komine et al., showed that in young men who had engaged in regular running exercise for ~80 min/day, 5 days/week for 6-7 years showed increases in arterial baroreflex gain through changes in the neural component of the baroreflex arc and not through alterations in carotid artery compliance [16]. Similarly, Deley showed that among previously sedentary elderly men and women, participation in a regular aerobic training program involving treadmill, elliptical training, and bicycle exercise at 70-80% heart rate reserve for six months enhanced baroreflex gain by 26%. The improvement in baroreflex gain was directly related to the amount of exercise performed and was derived primarily from changes in the neural component [36].

4.3 Effects of posture

Baroreflex function testing is generally conducted in the supine position. However, there are many activities in day-to-day living that produce physiological challenges and that have been associated with changes in baroreflex function, such as the assumption of an upright posture.[37] The risk of vasovagal syncope is greatly increased in the morning,[38] which may be associated with insufficient baroreflex function to maintain adequate blood pressure during orthostatic stress.[39] A number of studies have been performed to investigate the effects of orthostatic stress on integrated baroreflex function. The current consensus is that orthostatic stress augments vascular sympathetic gainand reduces cardio-vagal.[37, 40] Saeed et al., have provided further insight by showing that the differences in observed integrated BRS primarily arise from reduced mechanical transduction. These studies suggest that the propensity to orthostatic intolerance may be greater in those with structural vascular disease that affect the mechanical transduction properties of the integrated baroreflex arc.[41]

4.4 Stress response and baroreceptor function

Greater blood pressor responses to mental stress have been associated with greater risk of cardiovascular events, including the development of hypertension, stroke, coronary artery disease (CAD). Although blunting of baroreceptor function may underpin the exaggerated pressure responses associated with mental stress, the mechanisms underpinning the baroreceptor dysfunction are poorly understood. Deley et al., recently studied the mechanical and neural component of the baroreflex among healthy individuals and patients with documented coronary artery disease during the performance of a mental arithmetic and speaking task [42]. However, whilst patients with CAD showed exaggerated heart rate and blood pressure responses to the tasks, there were no differences in integrated, mechanical or neural baroreflex gains between healthy and CAD patients, which suggests that the augmented pressure response does not result from generalised baroreflex dysfunction.

4.5 Post exercise depression of baroreflex function

A single bout of moderate to high intensity exercise is associated with a period of post-exercise hypotension. Although the underlying cause of the hypotension remains unclear, studies have shown that following exercise in borderline hypertensive and young healthy subjects the integrated cardiac baroreflex gain changes dynamically. This change is characterised by an initial reduction [43] or no change [44] shortly after exercise (10-30 minutes), followed by elevation above baseline levels 40-55 minutes post exercise cessation. However, although these results clearly indicate that cardiac baroreflex function is altered during the post-exercise period, details regarding the sites and mechanisms underlying the changes remain entirely unknown.

Recently we examined for the first time the changes in cardiac baroreflex function before and at 10, 30, and 60 minutes after 40 minutes of cycling at 60% estimated maximal oxygen consumption.[45] We found that following aerobic exercise baroreflex gain is reduced and hysteresis manifests. The reduction in baroreflex gain to falling blood pressure is mediated by decreased mechanical and neural gains, whereas the decreased baroreflex gain to rising blood pressure is mediated by a reduced mechanical gain only. These findings indicate that impaired neural transduction of the cardiac baroreflex plays an important role in transient autonomic dysfunction after exercise that account for the increased propensity for syncope in the period immediately post exercise.

4.6 Diurnal variations in baroreflex function

We applied the technique to further understand the mechanisms underlying circadian variation in blood pressure, which exhibit a characteristic 'morning surge' following waking that has been linked to higher incidence of cardiac and cerebrovascular events [46]. We have shown that 1) the morning rise in blood pressure is related to overall reductions in integrated baroreflex gain, 2) that for falling pressures the lower integrated gain in the morning was caused by reduced neural gain compared with the afternoon, and 3) for rising pressures the lower integrated gain in the morning was caused by reduced mechanical gain compared with the afternoon [25]. These unique findings hold the prospect of guiding the development of future treatment strategies aimed at lowering cardio- and cerebrovascular events that occur more frequently in the morning. For example, given increases in blood pressure such as those that occur in the morning, may predispose to cerebral haemorrhage [47], hypertensive patients may benefit most from clinical interventions that focus augmenting the mechanical component by enhancing vascular properties. Conversely, individuals suffering from orthostatic intolerance, for which the risk is also greatest in the morning [48], may benefit from interventions aimed at enhancing the neural component [49].

5. References

[1] Grundy SM, D'Agostino Sr RB, Mosca L, Burke GL, Wilson PW, Rader DJ, Cleeman JI, Roccella EJ, Cutler JA, Friedman LM. Cardiovascular risk assessment based on us cohort studies: Findings from a national heart, lung, and blood institute workshop. *Circulation*. 2001;104:491-496.

[2] La Rovere MT, Pinna GD, Hohnloser SH, Marcus FI, Mortara A, Nohara R, Bigger JT, Jr., Camm AJ, Schwartz PJ. Baroreflex sensitivity and heart rate variability in the

identification of patients at risk for life-threatening arrhythmias: Implications for clinical trials. *Circulation*. 2001;103:2072-2077.

[3] La Rovere MT, Pinna GD, Maestri R, Robbi E, Caporotondi A, Guazzotti G, Sleight P, Febo O. Prognostic implications of baroreflex sensitivity in heart failure patients in the beta-blocking era. *J Am Coll Cardiol*. 2009;53:193-199.

[4] Sykora M, Diedler J, Rupp A, Turcani P, Rocco A, Steiner T. Impaired baroreflex sensitivity predicts outcome of acute intracerebral hemorrhage. *Crit Care Med*. 2008;36:3074-3079.

[5] Sykora M, Diedler J, Turcani P, Hacke W, Steiner T. Baroreflex: A new therapeutic target in human stroke? *Stroke*. 2009

[6] Jordan D, Spyer KM. Brainstem integration of cardiovascular and pulmonary afferent activity. *Prog Brain Res*. 1986;67:295-314.

[7] Scharf SM, Pinsky MR, Magder S. Heart-lung interactions. In: Scharf sm, pinsky mr, magder s, editors, respiratory-circulatory interactions in health and disease. Marcel dekker, new york, basel. 2001:1-7.

[8] Nosaka S, Yamamoto T, Yasunaga K. Localization of vagal cardioinhibitory preganglionic neurons with rat brain stem. *J Comp Neurol*. 1979;186:79-92.

[9] Gunn CG, Sevelius G, Puiggari J, Myers FK. Vagal cardiomotor mechanisms in the hindbrain of the dog and cat. *Am J Physiol*. 1968;214:258-262.

[10] Calaresu FR, Faiers AA, Mogenson GJ. Central neural regulation of heart and blood vessels in mammals. *Prog Neurobiol*. 1975;5:1-35.

[11] Fritsch JM, Smith ML, Simmons DT, Eckberg DL. Differential baroreflex modulation of human vagal and sympathetic activity. *Am J Physiol*. 1991;260:R635-641.

[12] Casadei B, Meyer TE, Coats AJ, Conway J, Sleight P. Baroreflex control of stroke volume in man: An effect mediated by the vagus. *J Physiol*. 1992;448:539-550.

[13] Eckberg DL, Kifle YT, Roberts VL. Phase relationship between normal human respiration and baroreflex responsiveness. *J Physiol*. 1980;304:489-502.

[14] Fisher JP, Kim A, Young CN, Ogoh S, Raven PB, Secher NH, Fadel PJ. Influence of ageing on carotid baroreflex peak response latency in humans. *J Physiol*. 2009;587:5427-5439.

[15] Hunt BE, Fahy L, Farquhar WB, Taylor JA. Quantification of mechanical and neural components of vagal baroreflex in humans. *Hypertension*. 2001;37:1362-1368.

[16] Komine H, Sugawara J, Hayashi K, Yoshizawa M, Yokoi T. Regular endurance exercise in young men increases arterial baroreflex sensitivity through neural alteration of baroreflex arc. *J Appl Physiol*. 2009;106:1499-1505.

[17] Saeed M, Link MS, Mahapatra S, Mouded M, Tzeng D, Jung V, Contreras R, Swygman C, Homoud M, Estes NA, 3rd, Wang PJ. Analysis of intracardiac electrograms showing monomorphic ventricular tachycardia in patients with implantable cardioverter-defibrillators. *Am J Cardiol*. 2000;85:580-587.

[18] Eckberg DL. Point:Counterpoint: Respiratory sinus arrhythmia is due to a central mechanism vs. Respiratory sinus arrhythmia is due to the baroreflex mechanism. *J Appl Physiol*. 2009;106:1740-1742.

[19] Karemaker JM. Counterpoint: Respiratory sinus arrhythmia is due to the baroreflex mechanism. *J Appl Physiol*. 2009;106:1742-1743.

[20] Smyth HS, Sleight P, Pickering GW. Reflex regulation of arterial pressure during sleep in man. A quantitative method of assessing baroreflex sensitivity. *Circ Res*. 1969;24:109-121.
[21] Diaz T, Taylor JA. Probing the arterial baroreflex: Is there a 'spontaneous' baroreflex? *Clin Auton Res*. 2006;16:256-261.
[22] Lipman RD, Salisbury JK, Taylor JA. Spontaneous indices are inconsistent with arterial baroreflex gain. *Hypertension*. 2003;42:481-487.
[23] Tzeng YC, Sin PY, Lucas SJ, Ainslie PN. Respiratory modulation of cardiovagal baroreflex sensitivity. *J Appl Physiol*. 2009;107:718-724.
[24] Studinger P, Goldstein R, Taylor JA. Mechanical and neural contributions to hysteresis in the cardiac vagal limb of the arterial baroreflex. *J Physiol*. 2007;583:1041-1048.
[25] Taylor CE, Atkinson G, Willie CK, Jones H, Ainslie PN, Tzeng YC. Diurinal variation in the mechanical and neural component of the baroreflex. *Hypertension*. 2011;Under review
[26] Hunt BE, Farquhar WB. Nonlinearities and asymmetries of the human cardiovagal baroreflex. *Am J Physiol Regul Integr Comp Physiol*. 2005;288:R1339-1346.
[27] Leitch JW, Newling R, Nyman E, Cox K, Dear K. Limited utility of the phenylephrine-nitroprusside sigmoid curve method of measuring baroreflex function after myocardial infarction. *J Cardiovasc Risk*. 1997;4:179-184.
[28] Ler AS, Cohen MA, Taylor JA. A planar elliptical model of cardio-vagal hysteresis. *Physiol Meas*. 2010;31:857-873.
[29] Vallbo AB, Hagbarth KE, Torebjork HE, Wallin BG. Somatosensory, proprioceptive, and sympathetic activity in human peripheral nerves. *Physiol Rev*. 1979;59:919-957.
[30] Studinger P, Goldstein R, Taylor JA. Age- and fitness-related alterations in vascular sympathetic control. *J Physiol*. 2009;587:2049-2057.
[31] Hart EC, Joyner MJ, Wallin BG, Karlsson T, Curry TB, Charkoudian N. Baroreflex control of muscle sympathetic nerve activity: A nonpharmacological measure of baroreflex sensitivity. *Am J Physiol Heart Circ Physiol*. 2010;298:H816-822.
[32] Kamiya A, Iwase S, Kitazawa H, Mano T, Vinogradova OL, Kharchenko IB. Baroreflex control of muscle sympathetic nerve activity after 120 days of 6 degrees head-down bed rest. *Am J Physiol Regul Integr Comp Physiol*. 2000;278:R445-452.
[33] Electrophysiology TFotESoCatNASoPa. Heart rate variability: Standards of measurement, physiological interpretation and clinical use. *Circulation*. 1996;93:1043-1065.
[34] Kamiya A, Kawada T, Shimizu S, Sugimachi M. Closed-loop spontaneous baroreflex transfer function is inappropriate for system identification of neural arc but partly accurate for peripheral arc: Predictability analysis. *J Physiol*. 2011;589:1769-1790.
[35] Halliwill JR, Taylor JA, Hartwig TD, Eckberg DL. Augmented baroreflex heart rate gain after moderate-intensity, dynamic exercise. *Am J Physiol*. 1996;270:R420-426.
[36] Deley G, Picard G, Taylor JA. Arterial baroreflex control of cardiac vagal outflow in older individuals can be enhanced by aerobic exercise training. *Hypertension*. 2009;53:826-832.
[37] O'Leary DD, Kimmerly DS, Cechetto AD, Shoemaker JK. Differential effect of head-up tilt on cardiovagal and sympathetic baroreflex sensitivity in humans. *Exp Physiol*. 2003;88:769-774.

[38] Mineda Y, Sumiyoshi M, Tokano T, Yasuda M, Nakazato K, Nakazato Y, Nakata Y, Yamaguchi H. Circadian variation of vasovagal syncope. *J Cardiovasc Electrophysiol*. 2000;11:1078-1080.

[39] Cooper VL, Hainsworth R. Effects of head-up tilting on baroreceptor control in subjects with different tolerances to orthostatic stress. *Clin Sci (Lond)*. 2002;103:221-226.

[40] Taylor JA, Eckberg DL. Fundamental relations between short-term rr interval and arterial pressure oscillations in humans. *Circulation*. 1996;93:1527-1532.

[41] Saeed NP, Reneman RS, Hoeks AP. Contribution of vascular and neural segments to baroreflex sensitivity in response to postural stress. *J Vasc Res*. 2009;46:469-477.

[42] Deley G, Lipman RD, Kannam JP, Bartolini C, Taylor JA. Stress responses and baroreflex function in coronary disease. *J Appl Physiol*. 2009;106:576-581.

[43] Somers VK, Conway J, LeWinter M, Sleight P. The role of baroreflex sensitivity in post-exercise hypotension. *J Hypertens Suppl*. 1985;3:S129-130.

[44] Halliwill JR, Taylor JA, Eckberg DL. Impaired sympathetic vascular regulation in humans after acute dynamic exercise. *J Physiol*. 1996;495 (Pt 1):279-288.

[45] Willie CK, Ainslie PN, Taylor CE, Jones H, Sin PY, Tzeng YC. Neuromechanical features of the cardiac baroreflex after exercise. *Hypertension*. 2011;57:927-933.

[46] Elliott WJ. Circadian variation in the timing of stroke onset: A meta-analysis. *Stroke*. 1998;29:992-996.

[47] Muller JE, Tofler GH, Willich SN, Stone PH. Circadian variation of cardiovascular disease and sympathetic activity. *J Cardiovasc Pharmacol*. 1987;10 Suppl 2:S104-109; discussion S110-101.

[48] Lewis NC, Atkinson G, Lucas SJ, Grant EJ, Jones H, Tzeng YC, Horsman H, Ainslie PN. Diurnal variation in time to presyncope and associated circulatory changes during a controlled orthostatic challenge. *Am J Physiol Regul Integr Comp Physiol*. 2010;299:R55-61.

[49] Thomas KN, Burgess KR, Basnyat R, Lucas SJ, Cotter JD, Fan JL, Peebles KC, Lucas RA, Ainslie PN. Initial orthostatic hypotension at high altitude. *High Alt Med Biol*. 2010;11:163-167.

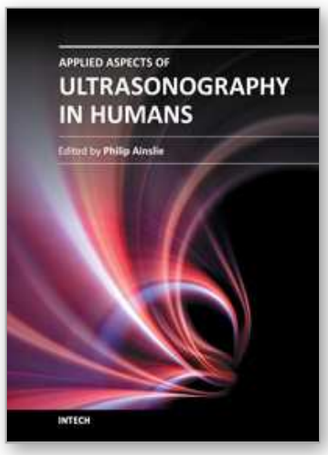

Applied Aspects of Ultrasonography in Humans
Edited by Prof. Philip Ainslie

ISBN 978-953-51-0522-0
Hard cover, 190 pages
Publisher InTech
Published online 25, April, 2012
Published in print edition April, 2012

Written by international experts, this publication provides the reader with the present knowledge and future research directions of diagnostic and therapeutic ultrasound and spectroscopy. Focused topics include Duplex ultrasound, transcranial color Duplex, MRA guided Doppler ultrasonography and near-infrared spectroscopy. New directions in the use and application of transcranial and color Duplex ultrasound are provided, as well as the use of ultrasound and arterial stiffness for measuring human vascular health and circulatory control. Novel use of ultrasound for the detection of intra-cardiac and intra-pulmonary shunts is also described along with its utility for the assessment of gastric regulation and emptying.

InTech Europe
University Campus STeP Ri
Slavka Krautzeka 83/A
51000 Rijeka, Croatia
Phone: +385 (51) 770 447
Fax: +385 (51) 686 166
www.intechopen.com

InTech China
Unit 405, Office Block, Hotel Equatorial Shanghai
No.65, Yan An Road (West), Shanghai, 200040, China
中国上海市延安西路65号上海国际贵都大饭店办公楼405单元
Phone: +86-21-62489820
Fax: +86-21-62489821

IntechOpen